ELSEVIER

Thin Solid Films 308–309 (1997) 594–598

thin Solid films

Characterization of TiN film grown by low-pressure-chemical-vapor-deposition

Y.J. Mei[a,*], T.C. Chang[b], J.C. Hu[c], L.J. Chen[c], Y.L. Yang[b], F.M. Pan[b], W.F. Wu[b], A. Ting[d], C.Y. Chang[a]

[a]*Department of Electronics Engineering and Institute of Electronics, National Chiao Tung University, 1001 Ta-Hsueh Rd., Hsin-Chu 300, Taiwan*
[b]*National Nano Device Laboratory, 1001 Ta-Hsueh Rd., Hsin-Chu 300, Taiwan*
[c]*Department of Material Science and Engineering, National Tsing Hua University, Hsin-Chu 300, Taiwan*
[d]*Materials Research Corporation, Hsin-Chu 300, Taiwan*

Abstract

Conformal TiN films were deposited by thermal low-pressure-chemical-vapor-deposition (LPCVD) in a rotating disk reactor, using $TiCl_4$ and NH_3 with N_2 as a dilution gas. TiN plug with 0.05 μm contact size was achieved. No void formation was observed in the TiN plug. The result demonstrated that LPCVD-TiN can be used to fill very small contact holes. The excellent step coverage and uniformity resulted from a surface-reaction-rate-limited deposition. The resistivity of TiN film was reduced to 133 $\mu\Omega$cm by in-situ NH_3 plasma post-treatment. The concentration of chlorine in the TiN film was measured to be less than 2 atomic % (at.%) by Auger electron spectroscope measurement. For Al deposited on TiN, the Al orientation was found to be dependent on the deposition method of Al film, but not on the underlying TiN orientation. © 1997 Elsevier Science S.A.

Keywords: TiN film; Low-pressure-chemical-vapour-deposition

1. Introduction

The microelectronics industry had shown an increasing interest in TiN because of its high thermal stability, low electrical resistivity, and good diffusion barrier characteristics [1–3]. As device dimensions scale down to deep submicron level, the limitation of films produced by physical vapor deposition has become apparent. Low-pressure-chemical-vapor-deposition (LPCVD) of TiN films provided excellent step coverage and uniformity [4,5] for 0.5 μm or even smaller contact windows. The improved feature was attributed to favorable surface controlled reactions. Generally, when chemical vapor deposition occurred in the surface-reaction-rate-limited regime, excellent step coverage was achieved.

Two organometallic precursors of tetrakis dimethyl amino titanium (TDMAT) [6] and tetrakis diethyl amino titanium (TDEAT) [7] were used to deposit CVD TiN film. However, deposition of MOCVD TiN by thermal decomposition of TDMAT and TDEAT would result in high carbon content. Carbon inclusion could be reduced by the organometallic with NH_3. However, it was difficult to eliminate carbon content. Thus, resistivity of MOCVD-TiN film was too high. By using $TiCl_4$ and NH_3 as reactants, with N_2 as a dilution gas, CVD-TiN films could be used as a diffusion barrier for Al interconnects and an adhesion layer for W-plugs. In the $TiCl_4/NH_3$-based CVD-TiN process, the incorporation of a significant amount of chlorine in the film is of major concern for long-term reliability of the finished device. However, Suzuki et al. reported that a higher deposition temperature (>600°C) could reduce Cl concentration in conventional thermal CVD-TiN film [8]. Hence, it appeared that a higher deposition temperature CVD process would suppress corrosion between Al and TiN. As a result, LPCVD TiN film could be used as a barrier layer between Si and Al interconnections. In addition, it was reported that Al film with (111) preferred orientation deposited onto TiN film could improve the electromigration resistance [9,10].

In this work, conformal TiN films were deposited by thermal LPCVD in a rotating disk reactor, using $TiCl_4$ and NH_3, with N_2 as a dilution gas. TiN plug with 0.05 μm contact size was achieved. In order to reduce the chlorine

* Corresponding author.

PII S0040-6090(97)00493-8

content of TiN film, an in-situ NH_3 plasma post-treatment was applied to as-deposited TiN film.

2. Experimental procedures

Single crystal, 15–25 Ωcm, 6-inch diameter, p-type (001) orientated silicon wafers were used in this work. The wafers were first cleaned by a standard RCA wet cleaning process. After initial cleaning, a 500 nm field of SiO_2 was thermally grown at 1050°C. Electron beam lithography (EBL) process and reactive ion etching (RIE) were used to open a pattern of silicon dioxide. Finally the wafers were dipped in a dilute HF solution (HF/H_2O, 1:50) immediately before loading into the deposition chamber. All the films were deposited by CVD processed in an MRC Multichamber cluster tool. The plasma-enhanced-chemical-vapor-deposition titanium (PECVD-Ti) chamber was utilized. The base vacuum level of the CVD chamber was maintained to be better than 10^{-6} Torr. Total pressure was fixed at 20 Torr when LPCVD TiN film was deposited. TiN films were deposited by LPCVD on SiO_2 (500 nm)/Si using $TiCl_4$ and NH_3 as reactants, with N_2 as a carrier gas. In addition, PECVD-Ti and LPCVD-TiN were deposited on the Si substrate in sequence. The substrate temperature during TiN film growth was maintained at 630°C. The in-situ NH_3 plasma post-treatment was applied to as-deposited TiN film. RF power of NH_3 plasma post-treatment was 500 W. Thermally-evaporated Al and sputtered-hot Al were also deposited to evaluate the crystal orientation of Al on $TiN/SiO_2/Si$.

A transmission electron microscope (TEM) and X-ray diffractometer (XRD) were utilized to investigate the microstructure and crystal orientation of these TiN films. Auger electron spectrocope (AES) was applied to determine the stoichiometry and uniformity down through the film. Thickness and N content of TiN films were measured by X-ray fluorescence (XRF). The morphology and step coverage were studied by a field-emission-scanning-electron-microscope (FESEM).

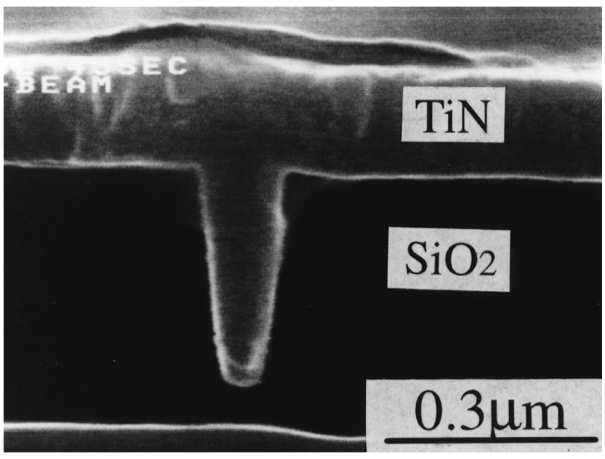

Fig. 1. Cross-section SEM image of TiN plug with 0.05 μm on the bottom and 0.1 μm on the top.

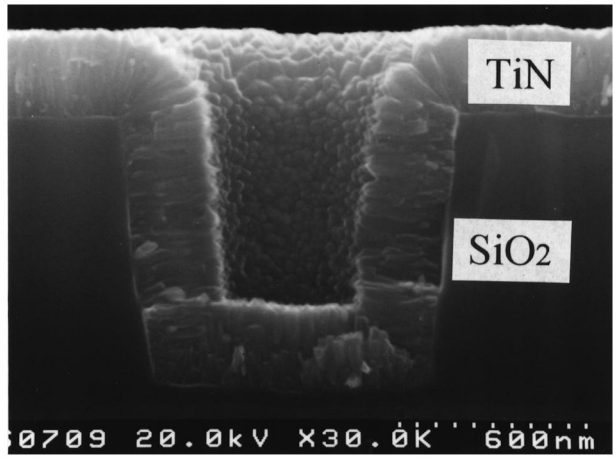

Fig. 2. Cross-section SEM image of TiN film on a 0.8 μm contact hole.

3. Results and discussion

TiN films were deposited by LPCVD on SiO_2 (500 nm)/Si, followed by in-situ NH_3 post-annealing for 30 s at 630°C. Flow rates of reactants and carrier gas were $TiCl_4$:42 scm, NH_3:78 sccm and N_2:3000 sccm, respectively. Fig. 1 shows a cross-section SEM image of a TiN plug of sizes 0.05 μm and 0.1 μm on the bottom or top, respectively. The thickness of the TiN film was 135 nm and the aspect ratio of the plug was 5.5. No void formation was evident in the TiN plug. This is the first preparation of a TiN plug with such a small dimension. This result indicated that the LPCVD-TiN can be used to fill very small contact hole. Excellent step coverage of 100% of the TiN film was revealed in Fig. 2. The superior characteristics of CVD-TiN films over those of PVD-TiN films were attributed to favorable surface-controlled reaction. Thin film XRD pattern of TiN film revealed a NaCl-like polycrystalline phase. A strong (002) orientation peak of TiN film was observed by XRD.

A cross-section TEM (XTEM) image of TiN film is seen in Fig. 3. The TiN films were found to be rather uniform.

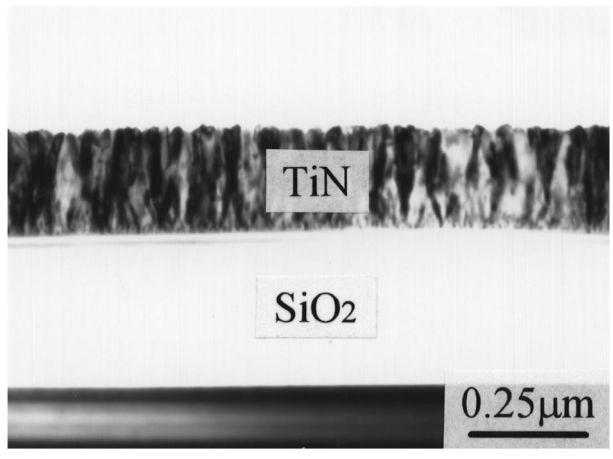

Fig. 3. XTEM image of TiN film formed by NH_3 post-annealing for 30 s at 630°C.

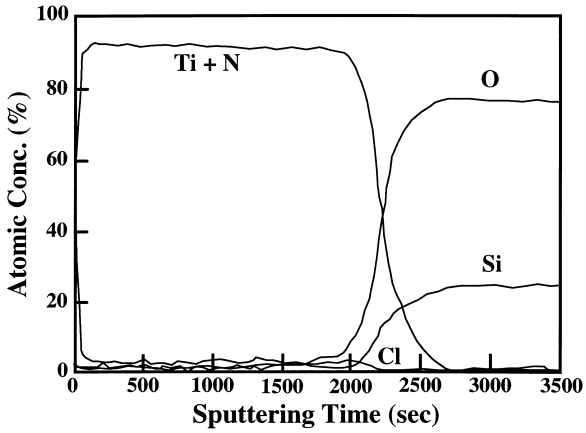

Fig. 4. AES depth profile of $TiN/SiO_2/Si$ sample.

The grains of TiN film were of columnar structure. No cracks were observed in the TiN films. Fig. 4 shows the AES depth profile of the TiN film which indicated that the chlorine is concentrated at the TiN/SiO_2 interface. It is thought that at a high deposition temperature (630°C) the majority of chlorine is trapped at the interface. On the other hand, the chlorine and the oxygen concentrations were low in the TiN film. A previous study showed that chlorine content in excess of 5 at.% would degrade metal reliability and increase resistivity of TiN film [9,10]. The content of chlorine in the deposited TiN film was 2.4 at.%, to minimize corrosion of the Al film.

The deposition rate of LPCVD-TiN as a function of $TiCl_4$ flow rate is shown in Fig. 5. $TiCl_4$ flow rates were 10, 14, 18, 20, 30 and 42 sccm, respectively. The NH_3 flow rate was kept at 78 sccm. The growth pressure and the temperature of reactor were fixed at 20 Torr and at 630°C, respectively. The deposition rate of TiN film had a complicated dependence on $TiCl_4$ concentration. Namely, if the $TiCl_4$ concentration was increased, the deposition rate increased rapidly, went through a maximum, and then slowly decreased. This behavior can be attributed to a surface-reaction-controlled process. At high $TiCl_4$ concentrations the surface was nearly

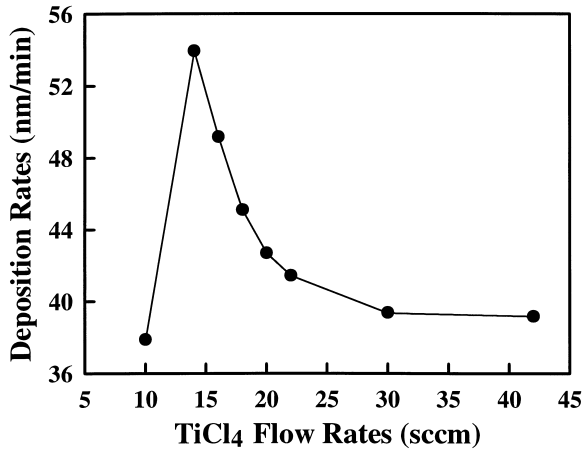

Fig. 5. Deposition rates of LPCVD-TiN as a function of $TiCl_4$ flow rates.

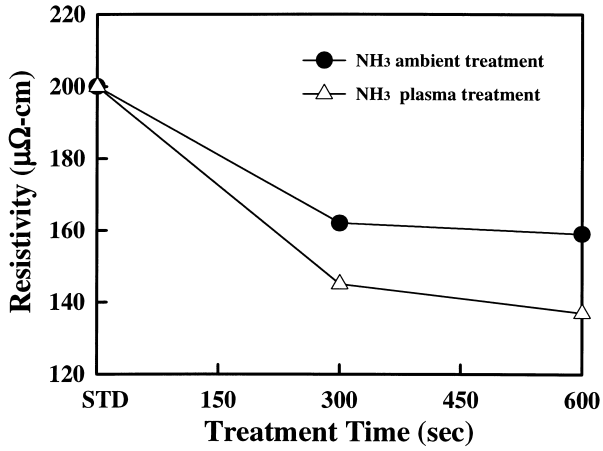

Fig. 6. Resistivity of samples as a function of the two post-treatment methods.

saturated with adsorbed $TiCl_4$ and further deposition blocked reaction with NH_3. As a result, the surface-reaction-rate-limited regime provided both excellent step coverage and uniformity, as shown in Figs. 2 and 3. In addition, the etching effect of chlorine at a high $TiCl_4$ flow rate may reduce the deposition rate of the LPCVD-TiN film. The deposition rate was about 40 nm/min and no appreciable incubation time was evident. The *x*-values of TiN_x with different flow rates were kept between 0.92 and 0.98, the films being characterized by XRF.

PECVD-Ti and LPCVD-TiN were also deposited on the Si substrate in sequence. The substrate temperature during Ti and TiN film growth was maintained at 630°C. $TiCl_4$ and H_2 were used as reaction gases during PECVD-Ti growth. A C49-$TiSi_2$ thin film, 9.5 nm in thickness, was directly formed from PECVD-Ti with Si substrate. Then a CVD-TiN thin film, 46 nm thick, was deposited on $TiSi_2/Si$. Both in-situ NH_3 post-annealing and in-situ NH_3 plasma post-treatment were carried out. The temperature for both post-treatments was kept at 630°C, which is the same as the deposition temperature. Fig. 6 shows the resistivity of these samples as a function of the two post-treatment times. The

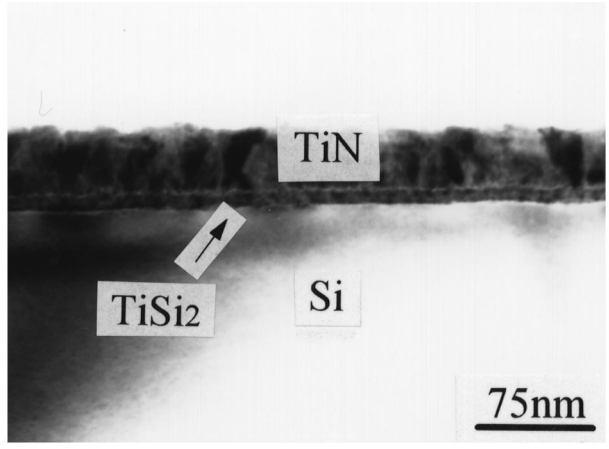

Fig. 7. XTEM image of $TiN/TiSi_2/Si$ sample treated by in-situ NH_3 plasma for 600 s.

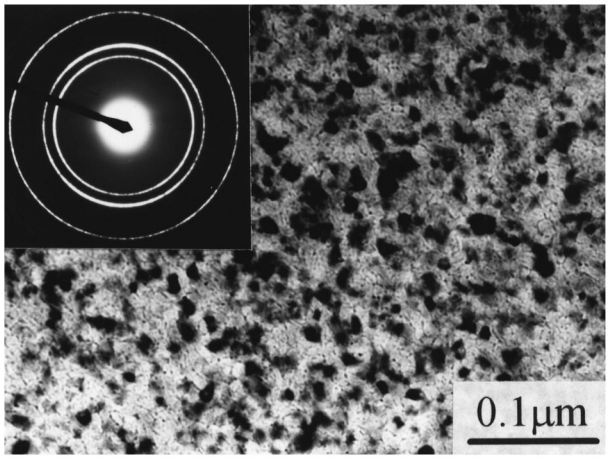

Fig. 8. Planview image and diffraction pattern of TiN sample treated by in-situ NH_3 plasma for 600 s.

resistivity of these samples decreased with the time of NH_3 post-annealing and that of NH_3 plasma post-treatment. The resistivity of these films was reduced from 200 $\mu\Omega$cm to 133 $\mu\Omega$cm after NH_3 plasma-treatment for 600 s. However, the resistivity of these films was only reduced to 160 $\mu\Omega$cm after annealing in NH_3 under ambient conditions. Therefore, in-situ NH_3 plasma post-treatment was found to be more effective in reducing the resistivity of TiN films.

A cross-section TEM image of TiN film treated by NH_3 plasma for 600 s is shown in Fig. 7. The interfaces of the $TiN/TiSi_2/Si$ structure are seen to be rather smooth. Planview micrograph and corresponding diffraction pattern are shown in Fig. 8. The average grain size of TiN film was found to be about 20 nm. Fig. 9 showed the AES depth profile of $TiN/TiSi_2/Si$ after being treated by NH_3 plasma for 600 s. The content of Cl in the sample was found to be very low (1.4 at.%) and fairly uniform,.

The electromigration resistance of Al alloy lines was previously reported to be strongly influenced by the aluminium texture [9,10]. Stronger (111) orientation of TiN film was preferred to (002) TiN films since their crystallographic

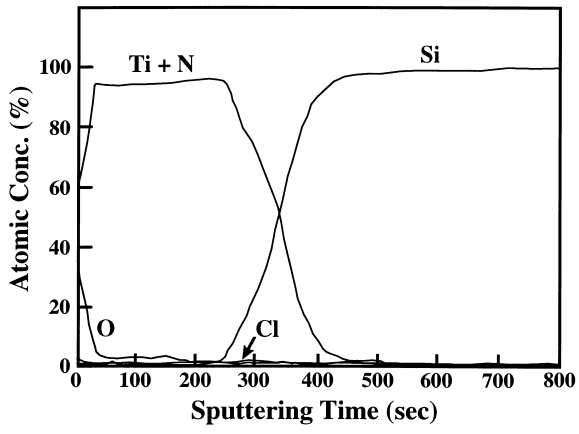

Fig. 9. AES depth profile of $TiN/TiSi_2/Si$ sample treated by in-situ NH_3 plasma for 600 s.

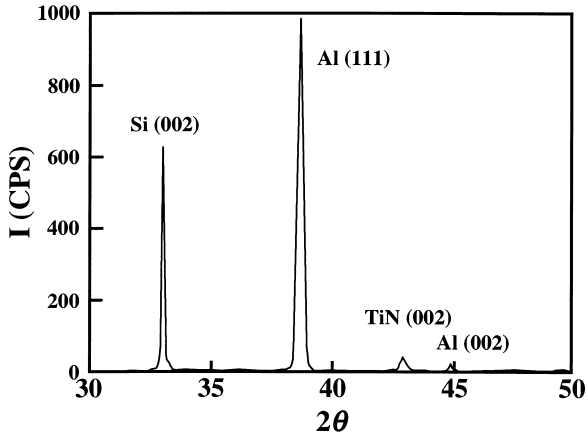

Fig. 10. The XRD patterns of thermally evaporated Al on (002) TiN film.

texture could transfer to Al films deposited onto TiN films. However, the transfer texture from TiN to Al was not observed in our work. We observed that the Al orientation was dependent on the deposition method of Al film. Figs. 10 and 11 show the XRD patterns of thermally-evaporated Al and sputtered hot Al on (002) TiN film, respectively. In Fig. 10, a small (002) peak and strong (111) peak of Al were seen. However, only one strong (111) peak of Al was evident in Fig. 11. This result suggested that the sputtered hot Al could have improved electromigration resistance.

4. Conclusions

Conformal TiN films were deposited by thermal LPCVD in a rotating disk reactor, using $TiCl_4$ and NH_3, with N_2 as a dilution gas. TiN plug with 0.05 μm contact size was achieved. No void formation was observed in the TiN plug. This result indicated that the LPCVD-TiN can be used to fill very small contact holes. In addition, deposition rates as a function of $TiCl_4$ flow rates were observed. The excellent step coverage, good uniformity and excellent plug-filling capability are attributed to a surface-reaction-

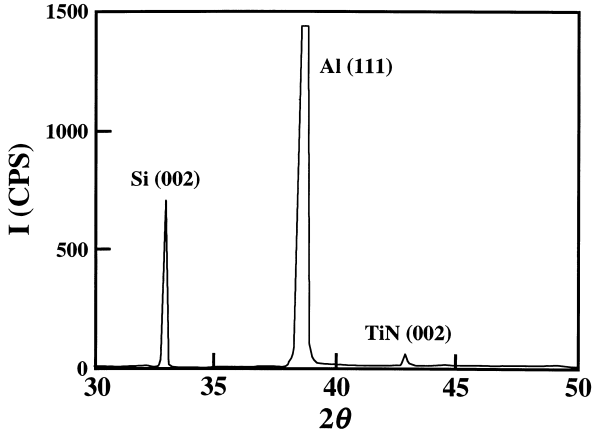

Fig. 11. The XRD patterns of sputtered hot Al on (002) TiN film.

rate-limited deposition. In-situ NH_3 plasma post-treatment was found to improve the electrical resistivity of the TiN films. The Cl content of LPCVD TiN film is rather low which avoids corrosion of Al films subsequently deposited. For Al deposited on TiN, the Al orientation was found to be dependent on the deposition method of the Al film, but not on TiN film orientation. Only one strong (111) orientation of sputtered hot Al was observed on the (002) TiN film. The result suggested that the sputtered hot Al has good electromigration resistance.

Acknowledgements

This work was performed at National Nano Device Laboratory and was supported by the National Science Council of Republic of China under contract NO. NSC86-2215-E317-003 and NO. NCS85-2721-2317-001.

References

[1] R.I. Hedge, R.W. Fiordalice, E.O. Travis and R.J. Tobin, *J. Vac. Sci. Technol. B, 11(4)* (1993) 1287.
[2] J.S. Byun, C.R. Kim, K.G. Rha and J.J. Kim, *Jpn. J. Appl. Phys., 34* (1995) 978.
[3] J.T. Hillman, R. Foster, J. Faguet, W. Triggs, R. Arora and M. Ameen, *Solid State Technol., 147* (1995).
[4] J.T. Hillman, *Proc. SEMI Taiwan Technical Conf.*, 1995, p. 8.
[5] J. Faguet, C. Arena, E. Guidotti, R.F. Foster and J.T. Hillman, *Advanced Metallization for ULSI Applications in 1995, Mater. Res. Stand.*, 1995, p. 259.
[6] A. Paranjpe and M.L. Raja, *J. Vac. Sci. Technol. B, 13* (1995) 2105.
[7] S.C. Sun and M.H. Tsai, *Thin Solid Films, 253* (1994) 440.
[8] T. Suzuki, T. Ohba, Y. Furumura and H. Tsutikawa, *Proc. 10th Int. VLSI Multilevel Interconnection Conf.*, IEEE, New York, 1993, p. 418.
[9] T. Kaizuka, H. Shinriki, N. Takeyasu and T. Ohta, *Jpn. J. Appl. Phys., 33* (1994) 470.
[10] R.W. Fiordalice, R.I. Hedge and H. Kawasaki, *J. Electrochem. Soc., 143* (1996) 2059.